L-shell spectroscopy of Au as a temperature diagnostic tool[a)]

E. Träbert,[b)] S. B. Hansen, P. Beiersdorfer, G. V. Brown, K. Widmann, and H.-K. Chung
High Temperature and Astrophysics Division, Lawrence Livermore National Laboratory, Livermore, California 94550-9234, USA

(Presented 12 May 2008; received 6 May 2008; accepted 19 May 2008; published online 31 October 2008)

In order to develop plasma diagnostic for reduced-size hot *Hohlraums* under laser irradiation, we have studied the *L*-shell emission from highly charged gold ions in the SuperEBIT electron beam ion trap. The resolving power necessary to identify emission features from individual charge states in a picket-fence pattern has been estimated, and the observed radiation features have been compared with atomic structure calculations. We find that the strong $3d_{5/2} \rightarrow 2p_{3/2}$ emission features are particularly useful in determining the charge state distribution and average ion charge $\langle Z \rangle$, which are strongly sensitive to the electron temperature. © *2008 American Institute of Physics.*
[DOI: 10.1063/1.2953443]

I. INTRODUCTION

One of the central goals of high-energy density physics is the production of a hot radiation environment, which can be used for studies of material under extreme conditions and possibly in local thermodynamic equilibrium (LTE). Recent experiments at the Omega laser at the University of Rochester's Laboratory for Laser Energetics or using the first four of the planned 196 beams of the National Ignition Facility at the Lawrence Livermore National Laboratory have demonstrated the production of radiation temperatures as high as 340 eV.[1,2]

The creation of extremely hot radiation environments requires depositing the available laser energy in the smallest possible space enclosed by walls of high-*Z* material (typically gold). The walls form a *Hohlraum* with a single opening, through which the laser light enters. The laser light is absorbed by the wall and ionizes the wall material. The resulting plasma reradiates a large fraction of the deposited laser energy and thus fills the *Hohlraum* with intense soft x-ray radiation.

Unlike the centimeter-size *Hohlraums* employed for inertial confinement fusion, reduced-size (submillimeter) "hot" *Hohlraums* fill with plasma on the time scale of the duration of the laser pulse. Plasma even spills out of the laser entrance hole (LEH) and interacts with the incoming laser light, partly blocking the entrance hole and thus limiting the amount of laser energy that can be deposited inside.[1,2] Hydrodynamic calculations have predicted electron densities of $n_e \approx 10^{21}$ cm^{-3} and electron temperatures from around 20 up to 30 keV in the plasma outside the LEH.

The present investigation seeks to provide a solid experimental and theoretical basis for spectroscopic diagnostics of the plasma outside the LEH of hot *Hohlraums*. Through measurements of Au *L*-shell emission on EBIT, we find that the emission of high-*Z* neonlike and lower charge state ions is dominated by $3d_{5/2} \rightarrow 2p_{3/2}$ transitions which form a "picket-fence" pattern of features,[3,4] similar to observations on *M*-shell transitions of gold and tungsten.[5–7] The shape of this pattern depends on the abundance of the ions of each charge state, which depends in turn on the plasma conditions. Coupled with a collisional-radiative and spectral synthesis model, measurements of the *L*-shell emission can serve as a means for determining the average ionization state of the plasma and its electron temperature. Developing a reliable temperature diagnostic thus requires the following steps: measurements determining the positions of features from individual ions, assessment of the necessary spectral resolving power, investigation into potential overlap of features from different charge states, and the demonstration of a reliable collisional-radiative model based on accurate atomic data.

An early implementation of *L*-shell Au spectroscopy for measuring the electron temperature off the LEH of a hot *Hohlraum* is given in measurements using the HENWAY spectrometer.[8] These measurements could not resolve individual x-ray lines. A high-resolution spectrometer has since been built which is capable of resolving the Au lines, as described at this conference.[9]

II. EXPERIMENT

The experiment was performed at the SuperEBIT electron beam ion trap[10] at the Lawrence Livermore National Laboratory. The device has been optimized for spectroscopic studies of highly charged ions.[11,12] X-ray emission from the ions in the trap was detected by means of a cryogenic microcalorimeter.[13] For single x-ray transitions at 8–10 keV, a linewidth (full width at half maximum) of about 10 eV was found, which implies a resolving power of about 900. Measured spectral features with larger line widths (15–18 eV) reveal the presence of line blends.

[a)]Contributed paper, published as part of the Proceedings of the 17th Topical Conference on High-Temperature Plasma Diagnostics, Albuquerque, New Mexico, May 2008.

[b)]Electronic mail: trabert1@llnl.gov. Also at Astronomisches Institut, Ruhr-Universität Bochum, D-44780 Bochum, Germany.

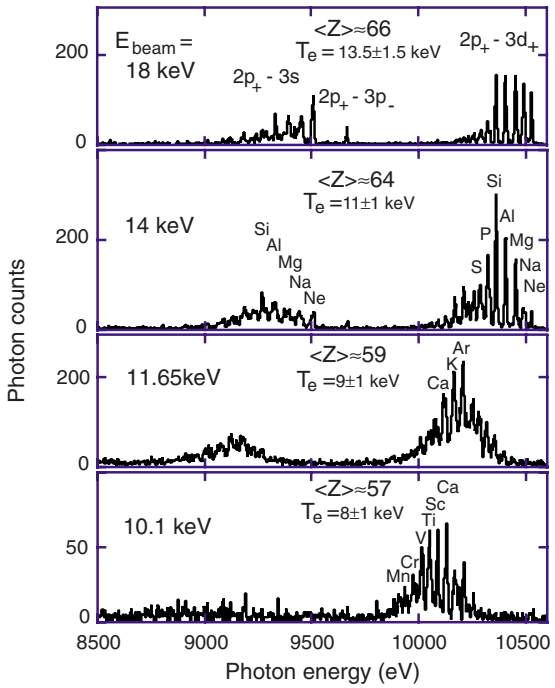

FIG. 1. (Color online) Measured *L*-shell Au emission at four electron beam energies. The prominent features are labeled according to their parent ion and transition type. The approximate average ion charges $\langle Z \rangle$ of the emission spectra are listed along with the electron temperatures that would be diagnosed by our collisional-radiative models given emission spectra with similar $\langle Z \rangle$ from a plasma with coronal conditions and $n_e = 10^{12}$ cm^{-3}.

The adjustable beam energy of the device allows us to step through the charge states, enabling unambiguous identification of the strong *L*-shell lines and line blends, in this experiment of Au^{53+} through Au^{69+} (Fe- through Ne-like ions). The highest charge state of interest was Au^{69+} (Ne like), with an ionization potential (IP) of 18 keV. The IPs of the next lower charge state ions are 8.4 keV and consecutively lower. However, the IP refers to the valence electron ($n=3$ for those ions below the Ne-like ion), whereas the x-ray transitions of present interest relate to inner-shell excitation.

An expanded view of a section of the microcalorimeter spectra (Fig. 1) shows the two to three emissions of the gold ions at various electron beam energies. The Au emission varies with the electron beam energy: as E_{beam} decreases, the intensity of major emission features shifts to lower energies. The picket-fence structure of the $3d_{5/2} \rightarrow 2p_{3/2}$ emission features in our spectra extends from neonlike Au^{69+} to ironlike Au^{53+}, with a picket-fence spacing of about 40 eV. The lower-energy line groups ($3d_{3/2} \rightarrow 2p_{3/2}$ and $3s_{1/2} \rightarrow 2p_{3/2}$) are weaker than the others for several reasons; statistical level population will be lower for the $j=3/2$ and $j=1/2$ levels than for $j=5/2$, and the competing autoionization decay branch (Auger effect) is much stronger.

The highest-energy peak of each line group belongs to the Ne-like ion. Line blending becomes significant for charge states below about Ti-like Au^{55+}; for those ions, full modeling is needed to predict the emission. However, in higher-temperature plasmas, where the average ion charge $\langle Z \rangle$ is well above 56+, the $3d_{5/2} \rightarrow 2p_{3/2}$ features provide a reasonably good indication of the charge balance even in the absence of detailed modeling. In this range, that is, for plasma temperatures of about 8 keV and higher, an instrument of resolving power $E/\Delta E \geqslant 400$ would be able to observe the picket-fence pattern and thus the charge state distribution (CSD).

III. ATOMIC STRUCTURE AND COLLISIONAL-RADIATIVE CALCULATIONS

We have used the flexible atomic code (FAC) of Gu[14] to generate fine-structure atomic levels and rate data for Au ions from H-like (Au^{78+}) to Zn-like (Au^{49+}). These data have enabled unambiguous association of strong *L*-shell emission features with particular ions, as the labels given in Fig. 1 demonstrate. We found ≈5 eV maximum discrepancy in transition energies between the FAC atomic structure calculations and the experimental measurements–a disagreement much smaller than the typical 40 eV separation of emission features from different charge states.

The FAC atomic structure and rate data were then used in the collisional-radiative and spectral synthesis code SCRAM to calculate level populations, CSDs, and emission spectra.[15] This version of SCRAM uses a hybrid atomic structure scheme to ensure both accuracy of atomic data in the coronal limit and completeness in the approach to LTE. For each ion, fine-structure energy levels and rates are calculated for a subset of configurations, then supplemented with relativistic configuration averaged levels (*nlj* terms) and superconfigurations. This hybrid atomic structure reproduces the results of the best "coronal" models, which are generally adequate to describe emission from low-density sources such as EBIT, where electronic state populations are overwhelmingly concentrated in ground state configurations and line emission tends to be limited by direct collisional excitation and ionization. It also performs well at higher densities, where multistep processes lead to significant population in multiply excited configurations, opening up new channels for population transfer and giving rise to strong satellite emission features. A key feature of the hybrid model is that it remains tractable even for complex ions because of its flexible structure. A second key feature is the extension of configuration interaction effects on transition energies and strengths from the fine-structure levels to the *nlj* terms.

The calculations show details of the spectra that the observations at their present resolution do not, but which are important for diagnostics: the $3d_{5/2} \rightarrow 2p_{3/2}$ spectral features have a substructure. For Mg- to V-like ions, a high-energy satellite feature almost coincides with the main lines of the next higher charge state. Beginning as a few-percent contribution, it grows into the dominant feature for ions with more than 23 electrons (V-like). There is also a weak substructure on the low-energy side that begins for ions with more electrons than about 20 (Ca-like, Au^{59+}) and coincides with the main features of ions two charge states down. The $3s_{1/2} \rightarrow 2p_{3/2}$ spectral features split up also, without a dominant line feature below Mg-like ions. The almost equally weak emission features of a given charge state partly overlap with those of neighboring charge states on either side, rendering these transitions impractical for diagnostics.

IV. DIAGNOSTIC FEATURES

The experimental data obtained from the combination of an electron beam ion trap with a microcalorimeter reveal the core-excitation spectra of Au at a resolution that clearly separates the dominant features from individual charge states. The calculated spectra, however, show more complexity and detail than the data do at the present resolution and suggest that only the $3d_{5/2} \rightarrow 2p_{3/2}$ transitions in Ne- to Ti-like ions make for a practical and rigorous diagnostic tool following a simple picket-fence radiation pattern.

We present elsewhere[16] detailed comparisons of modeled and measured spectra and systematic calculations of the average ion charge of Au ions at electron temperatures from 5 to 15 keV and electron densities n_e from 10 to 10^{22} cm^{-3}, using both the hybrid atomic structure code SCRAM and the screened hydrogenic code FLYCHK.[17] In the present paper, we have listed in Fig. 1 the electron temperatures that would be diagnosed given emission spectra from a plasma with $n_e = 10^{12}$ cm^{-3} and $\langle Z \rangle$ (or central wavelength) similar to those of the given EBIT spectra. The uncertainty in the diagnosed temperatures of $\approx 10\% - 15\%$ represents roughly the degree of disagreement between the two collisional-radiative models. At temperatures above 10 keV or densities below about 10^{19} cm^{-3}, our $\langle Z \rangle$ calculations are fairly insensitive to n_e. However, at lower temperatures and at densities near or above 10^{21} cm^{-3}, the calculated $\langle Z \rangle$ is sensitive to density, tending to increase with increasing n_e due to ladder ionization.

The line emission is also sensitive to density: as n_e increases, emission features from the complex M-shell ions broaden and can shift to lower energies by as much as 10 eV due to increasing populations in multiply excited configurations. This explains the results of an earlier beam-foil experiment,[18] where excitation takes place at high (near-solid) density: while their measured Ne-like line energies closely agree with our measurements, their Na- and Mg-like features have lower energies.

Increasing collisionality and Stark effects will also contribute to line broadening. For plasmas with significant Ne-like Au populations, the metastable line intensities provide another potential density diagnostic. With increasing densities, collisions tend to depopulate the upper level of weak forbidden lines that are fed by radiative cascades in low-density sources. Our calculations show that the $M2$ line disappears well before the density reaches 10^{21} cm^{-3} and that the $3G$ line begins to decrease significantly at an electron density near 10^{22} cm^{-3}.

ACKNOWLEDGMENTS

This work was performed under the auspices of the U.S. Department of Energy by Lawrence Livermore National Laboratory under Contract No. DE-AC52-07NA27344. G.B., H.K.C., S.B.H., and K.W. were supported in part by LLNL LDRD 05-erd-068. E.T. acknowledges travel support from the German Research Foundation (DFG).

[1] D. E. Hinkel, M. B. Schneider, H. A. Baldis, G. Bonanno, D. E. Bower, K. M. Campbell, J. R. Celeste, S. Compton, R. Costa, E. L. Dewald, S. N. Dixit, M. J. Eckart, D. C. Eder, M. J. Edwards, A. Ellis, J. A. Emig, D. H. Froula, S. H. Glenzer, D. Hargrove, C. A. Haynam, R. F. Heeter, M. A. Henesian, J. P. Holder, G. Holtmeier, L. James, K. S. Jancaitis, D. H. Kalantar, J. H. Kamperschroer, R. L. Kauffman, J. Kimbrough, R. K. Kirkwood, A. E. Koniges, O. L. Landen, M. Landon, A. B. Langdon, F. D. Lee, B. J. MacGowan, A. J. Mackinnon, K. R. Manes, C. Marshall, M. J. May, J. W. McDonald, J. Menapace, E. I. Moses, D. H. Munro, J. R. Murray, C. Niemann, D. Pellinen, V. Rekow, J. A. Ruppe, J. Schein, R. Shepherd, M. S. Singh, P. T. Springer, C. H. Still, L. J. Suter, G. L. Tietbohl, R. E. Turner, B. M. Van Wonterghem, R. J. Wallace, A. Warrick, P. Watts, F. Weber, P. J. Wegner, E. A. Williams, B. K. Young, and P. E. Young, Phys. Plasmas **12**, 056305 (2005).
[2] D. E. Hinkel, M. B. Schneider, B. K. Young, A. B. Langdon, E. A. Williams, M. D. Rosen, and L. J. Suter, Phys. Rev. Lett. **96**, 195001 (2006).
[3] P. Beiersdorfer, M. Bitter, S. von Goeler, S. Cohen, K. W. Hill, J. Timberlake, R. S. Walling, M. H. Chen, P. L. Hagelstein, and J. H. Schofield, Phys. Rev. A **34**, 1297 (1986).
[4] P. Beiersdorfer, S. von Goeler, M. Bitter, E. Hinnov, R. Bell, S. Bernabei, J. Felt, K. W. Hill, R. Hulse, J. Stevens, S. Suckewer, J. Timberlake, A. Wouters, M. H. Chen, J. H. Scofield, D. D. Dietrich, M. Gerassimenko, E. Silver, R. S. Walling, and P. L. Hagelstein, Phys. Rev. A **37**, 4153 (1988).
[5] M. J. May, K. B. Fournier, P. Beiersdorfer, H. Chen, and K. L. Wong, Phys. Rev. E **68**, 036402 (2003).
[6] P. Neill, C. Harris, A. S. Safronova, S. Hamasha, S. Hansen, U. I. Safronova, and P. Beiersdorfer, Can. J. Phys. **82**, 931 (2004).
[7] M. J. May, P. Beiersdorfer, N. Jordan, J. H. Scofield, K. J. Reed, S. B. Hansen, K. B. Fournier, M. F. Gu, G. V. Brown, F. S. Porter, R. Kelley, C. A. Kilbourne, and K. R. Boyce, Nucl. Instrum. Methods Phys. Res. B **235**, 231 (2005).
[8] M. J. May, M. B. Schneider, S. B. Hansen, H.-K. Chung, D. E. Hinkel, H. A. Baldis, and C. Constantin, "X ray Spectral Measurements and Collisional Radiative Modeling of Hot Plasmas at the Omega Laser," High Energy Density Phys. (submitted).
[9] K. Widmann, M. B. Schneider, H.-K. Chung, L. D. James, G. V. Brown, M. J. May, D. E. Hinkel, K. V. Cone, D. B. Thorn, P. Beiersdorfer, and H. A. Baldis, Rev. Sci. Instrum. (these proceedings).
[10] D. A. Knapp, R. E. Marrs, S. R. Elliott, E. W. Magee, and R. Zasadzinski, Nucl. Instrum. Methods Phys. Res. A **334**, 305 (1993).
[11] P. Beiersdorfer, Can. J. Phys. **86**, 1 (2008).
[12] M. B. Schneider, R. Mancini, K. Widmann, K. B. Fournier, G. V. Brown, H.-K. Chung, H. A. Baldis, K. Cone, S. B. Hansen, M. J. May, D. Thorn, and P. Beiersdorfer, Can. J. Phys. **86**, 259 (2008).
[13] F. S. Porter, P. Beiersdorfer, K. R. Boyce, G. V. Brown, H. Chen, J. Gygax, S. M. Kahn, R. L. Kelley, C. A. Kilbourne, E. Magee, and D. B. Thorn, Can. J. Phys. **86**, 231 (2008).
[14] M. F. Gu, Can. J. Phys. **86**, 675 (2008).
[15] S. B. Hansen, J. Bauche, C. Bauche-Arnoult, and M. F. Gu, High Energy Density Phys. **3**, 109 (2007).
[16] G. V. Brown, S. B. Hansen, E. Träbert, P. Beiersdorfer, K. Widmann, H. Chen, H. K. Chung, J. H. T. Clementson, M. F. Gu, and D. B. Thorn, Phys. Rev. E **77** 066406 (2008).
[17] H. K. Chung, M. H. Chen, W. L. Morgan, Y. Ralchenko, and R. W. Lee, High Energy Density Phys. **1**, 3 (2005).
[18] G. A. Chandler, M. H. Chen, D. D. Dietrich, P. O. Egan, K. P. Ziock, P. H. Mokler, S. Reusch, and D. H. H. Hoffmann, Phys. Rev. A **39**, 565 (1989).